Use of spectroscopy for assessment of color discrimination in animal vision

Derya Akkaynak[1,2,3]

[1]*Department of Mechanical Engineering, Massachusetts Institute of Technology, 77 Massachusetts Avenue, Cambridge, Massachusetts 02139, USA*
[2]*Applied Ocean Science and Engineering, Woods Hole Oceanographic Institution, 266 Woods Hole Road, Woods Hole, Massachusetts 02543, USA*
[3]*Program in Sensory Physiology and Behavior, Marine Biological Laboratory, 7 MBL Street, Woods Hole, Massachusetts 02543, USA (deryaa@mit.edu)*

Received October 3, 2013; accepted November 1, 2013;
posted November 14, 2013 (Doc. ID 198674); published December 19, 2013

Animals use color vision for a number of tasks including food localization, object recognition, communication, and mate selection. For these and other specific behaviors involving the use of color cues, models that quantify color discriminability have been developed. These models take as input the photoreceptor spectral sensitivities of the animal and radiance spectra of the surfaces of interest. These spectra are usually acquired using spectroscopic instruments that collect point-by-point data and can easily yield signals contaminated with neighboring colors if not operated carefully. In this paper, I present an equation that relates the optical fiber diameter and numerical aperture to the measurement angle and distance needed to record uncontaminated spectra. I demonstrate its utility by testing the discriminability of two solid colors for the visual systems of a dichromatic ferret and a trichromatic frog in (1) a conspicuous scenario where the colors have little spectral overlap and (2) a perfect camouflage scenario where the spectra are identical. This equation is derived from geometrical optics and is applicable to spectroscopic measurements in all fields.

OCIS codes: (300.0300) Spectroscopy; (300.6550) Spectroscopy, visible; (330.0330) Vision, color, and visual optics; (330.1710) Color, measurement; (330.1720) Color vision.
http://dx.doi.org/10.1364/JOSAA.31.000A27

1. INTRODUCTION

Color vision is the ability to distinguish surfaces based on their spectral properties [1]. In the field of animal biology, understanding animal color vision helps answer important scientific questions. For example, Maan and Cummings [2] found that for female poison frogs, the male's dorsal color is the only factor determining their choice of a mate. In addition to sexual selection, animals use color vision for behavioral tasks including finding food, recognizing objects, and communicating with members of the same species [3]. In order to accurately capture and interpret how color signals are received, we must have a model of the observer animal's visual system because analyzing color signals from the point of view of humans and making inferences about their appearances to animals often produce erroneous conclusions. For example, Stoddard and Stevens [4] showed that some common cuckoo eggs (which are laid in nests of other species and often hatched and raised by unsuspecting host birds) appeared to have a good color match to the host eggs when viewed by humans but had clear and quantifiable differences when modeled in avian color space. A detailed summary of how color signals can be modeled from the perspective of animals can be found in [5]. In this paper, my focus is not on these models but on the measurement of the color signals.

Color is inherently difficult to measure objectively because it is a sensation defined relative to the human visual system [6]. Visual systems of most other animals are different from that of humans, and analyses from the perspective of other systems must start with unfiltered spectral data encompassing the segment of the electromagnetic spectrum to which the animal is sensitive. Spectral information in a scene can be captured most comprehensively using a hyperspectral imager [7], which, for each pixel in its sensor, records a densely sampled portion of the electromagnetic spectrum. Despite providing spectral data for every pixel in an image, hyperspectral imagers are not commonly used in studies of animal coloration (or most other research fields). This is because they are still expensive, physically bulky, have low resolution, create large digital files, and are not fast enough for imaging moving objects (i.e., animals in the wild). Although consumer digital cameras are inexpensive, fast, compact, and widely available, they cannot serve as substitutes for hyperspectral imagers because they record spectral information with limited spectral resolution [7]. An intermediate solution is to use spectrometers, which are effectively single-pixel hyperspectral imagers. In the field of animal biology and coloration, spectrometers with optical fibers are frequently used to measure colors from an animal's habitat, nest, eggs, body parts, skin, fur, plumage, etc. Table 1 lists a subset of recent publications in which animal or habitat colors measured using spectrometers were simulated for other visual systems.

Spectrometers collect data in a point-by-point fashion, which means they are not suitable for recording color information from textured surfaces, i.e., those with high-frequency color or pattern elements. Even in the case of surfaces with solid colors and a carefully gridded, sequential data collection

Table 1. Recent Publications That Assess the Discriminability of Colors Based on Measurements Taken by Spectrometers[a]

Publication	Fiber Diameter, Distance, and Angle	Spectra Measured	Visual System Modeled
Chiao *et al.* [10]	Hyperspectral N/A	European cuttlefish	Fish
Isaac and Gregory [11]	100 μm, 2 mm, 90°	Western terrestrial garter snake	Ferret human birds
Akkaynak *et al.* [8]	50 and 100 μm, < 3 cm, N/A	European cuttlefish	Fish human
Hanlon *et al.* [9]	400 μm, 2 mm, N/A	Giant Australian cuttlefish	Fish
Finkbeiner *et al.* [12]	400 μm, N/A, 45°	Passion-vine butterflies	Birds
Lind *et al.* [13]	1000 μm, N/A, 45°	Blue tit	Birds
Maan and Cummings [14]	400 μm, 3 mm, 90°	Strawberry poison frog	Birds, crabs, snakes, frogs
Bybee *et al.* [15]	400 μm, N/A, 45°	Heliconius butterfly	Birds butterflies
Cortesi and Cheney [16]	200 μm, N/A, 45°	Marine *Opisthobranchs*	Fish
Langmore *et al.* [17]	N/A, N/A, 45°	Cuckoo eggshell	Birds
Baldwin and Johnsen [18]	400 μm, N/A, 45°	Blue crab	Blue crab
Nokelainen *et al.* [19]	N/A, N/A, 45°–90°	Wood tiger moth	Blue tit
Stoddard and Stevens [4]	N/A, N/A, 45°	Cuckoo eggs	Birds
Siddiqi *et al.* [20]	N/A, N/A, N/A	Strawberry poison frogs	Strawberry poison frogs

[a]Partial list.

setup, the distance of the optical fiber to the sample, its diameter, numerical aperture (NA), and the measurement angle could affect the purity of the color signal recorded. In general, it is known to researchers that measurements should be taken as close as possible to the surface being measured to avoid the contamination of the signal by neighboring colors, and this distance is usually reported in publications (Table 1). However, how close the optical fiber should be held relative to the size and shape of the feature being measured, and at what angle, is generally not quantified but assumed. It is important to know the optimum measurement distance because recording closely from live animals, especially in the wild, can be challenging [8,9], and it may be difficult to position the measuring fiber as close to the sample as it would have been possible in a laboratory setting (Fig. 1). In such cases, the spectra recorded may not be pure, and to assess data quality and prevent measurement errors, the degree of contamination should be known.

In this work, I develop an equation using geometrical optics that only depends on the diameter and the NA of the optical fiber and analyze the effect of the measurement distance and angle on the discriminability of colors in the eyes of a dichromatic ferret (*Mustela putorius furo*) and a trichromatic frog (*Dendrobates pumilio*). This equation is then tested on two cases relevant to animal biology: (1) colors that have little spectral overlap as an example of a conspicuous appearance, and (2) colors that have high spectral overlap as an example of a camouflage pattern.

2. FIELD OF VIEW OF AN OPTICAL FIBER

An optical fiber is a waveguide that propagates rays through total internal reflection [21]. It is a cylindrically symmetric cable with a core that has high refractive index n_{core} surrounded by cladding with low refractive index, n_{clad} (Fig. 2). Fibers are characterized by their NA, which is defined relative to the refractive index of the medium of operation (n_{med}) and the acceptance angle (θ_0) as

$$\text{NA} = n_{\text{med}} \cdot \sin \theta_0. \tag{1}$$

(a) (b)

Fig. 1. (a) Scuba diver extending the optical fiber attached to a spectrometer (in water and pressure proof housing) to record the spectrum of light reflected from the skin of a cuttlefish, in Urla, Turkey. Getting the optical fiber close enough to take accurate measurements from freely behaving animals in the wild is challenging. Image reproduced here with kind permission from Springer Science+Business Media: Journal of Comparative Physiology A, Quantification of cuttlefish (*Sepia officinalis*) camouflage: a study of color and luminance using *in situ* spectrometry, 199, 2013, 211–225, Fig. 1, photo credit: D. Akkaynak. (b) Spectral measurements of a specimen can be recorded in a laboratory by getting the fiber as close as possible to the specimen without touching it. Photo courtesy of M. C. Stoddard and K. Zyskowski, taken at the Ornithology Collections of the Peabody Museum of Natural History, Yale University, New Haven, Connecticut.

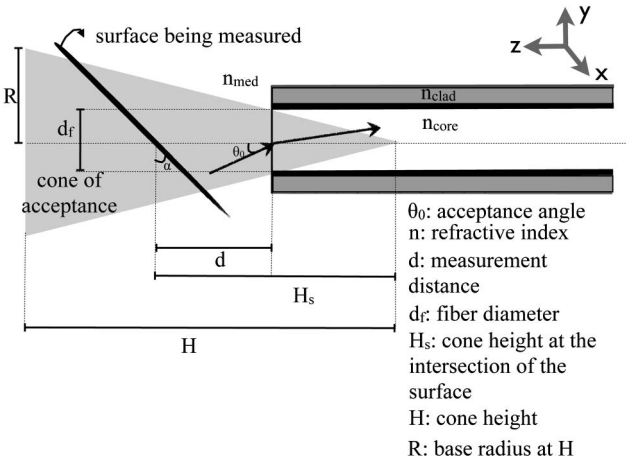

Fig. 2. Field of view of an optical fiber.

The acceptance angle is the largest incidence angle for incoming rays to undergo total internal reflection. The locus of all such rays is the cone of acceptance (shown in light gray in Fig. 2). For most animal biology applications, the optical fiber is used in air ($n_{\text{med}} \approx 1$), or water ($n_{\text{med}} \approx 1.33$); the difference between fresh and salt water is usually ignored for practical purposes. When the fiber is oriented along the z direction and is held at distance of d from a surface tilted at an angle α relative to the XY plane, the cross section of the acceptance cone on the surface is an ellipse (Fig. 2). In the trivial case when $\alpha = 0$, the plane will be parallel to the base of the cone, and the intersection of the cone and the plane will be a circle. In the general case (proof is given in Appendix A), for a fiber with diameter d_f and NA, the elliptical cross section is in the form

$$\frac{(x-x_c)^2}{a^2} + \frac{(y-y_c)^2}{b^2} = 1, \tag{2}$$

where

$$(x_c, y_c) = \left(0, \frac{H_S \tan\alpha}{\frac{1}{t^2} - (\tan\alpha)^2}\right) \tag{3}$$

are the coordinates of the center of the ellipse, and

$$a^2 = \frac{H_s^2 t^2}{\left(\frac{1}{t^2} - (\tan\alpha)^2\right)^2} \tag{4}$$

and

$$b^2 = \frac{a^2}{\frac{1}{t^2} - (\tan\alpha)^2} \tag{5}$$

are the squares of the semi-major and semi-minor axes, respectively. Here, it can be shown from geometry that $t = (R/H) = \tan(\sin^{-1}(\text{NA}/n_{\text{med}}))$. The height H_S is measured from the apex of the cone to the intersection of the surface and the axis of the optical fiber (Fig. 2) and is given by

$$H_S = d + \frac{d_f}{2\tan\left(\sin^{-1}\left(\frac{\text{NA}}{n_{\text{med}}}\right)\right)}. \tag{6}$$

3. APPLICATION TO ANIMAL COLOR DISCRIMINATION

In this section, the effect of the measurement distance and angle on the quality of the recorded spectral signals is investigated using the visual systems of a dichromatic ferret (*Mustela putorius furo*) and a trichromatic frog (*Dendrobates pumilio*). Fibers are assumed to have diameters 100, 400, and 1000 μm with NA = 0.22. The operation medium is air ($n_{\text{med}} = 1$) and the illuminant is CIE D65, which is a theoretical light spectrum that approximates noon daylight. Solid color patches of dimensions 4.1 cm × 4.1 cm (the actual size of patches on a Macbeth ColorChecker, Xrite, Inc.) on a synthetic test target are used to simulate two test cases relevant to animal coloration: (1) colors expected to yield high contrast (i.e., a conspicuous animal) and (2) colors expected to yield low contrast (i.e., a camouflaged animal).

A. Synthetic Test Stimuli

A synthetic test target was created to show the effect of sampling colors erroneously. The target was designed to have the same arrangement and patch size as a Macbeth ColorChecker, a standard in color calibration. Since Macbeth charts only provide tristimulus values, complete spectra from the METACOW project [22] were substituted for matching colors. The spectra were obtained by averaging the reflectance spectra of a 50 × 50 pixel region from the left half of each METACOW sample. The resulting stimulus was a hyperspectral calibration target with square patches of solid colors, each of which had reflectance spectra in the interval 400–700 nm in 5 nm steps (Fig. 3).

For case (1), spectra from patches A and B [Fig. 3(b)] were chosen to represent a conspicuous animal's pattern. The red and blue patches were expected to contrast highly for any visual system because they have little spectral overlap. To create a camouflaged animal that perfectly matches the colors of its background for case (2), the reflectance spectrum of patch A was copied onto the location of patch B, creating two neighboring patches that were identical. These patches would be expected to have minimal color contrast if the color was sampled without contamination from neighboring colors. Note that in both cases, there was a black border between the color patches (similar to the original Macbeth ColorChecker), which could affect the quality of the recorded signal.

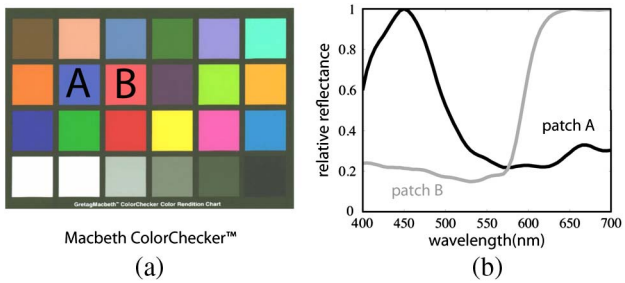

(a) (b)

Fig. 3. Test stimuli used for assessment of color discrimination for a conspicuous animal (case 1), and a camouflaged animal (case 2). (a) The synthetic hyperspectral test target has the same layout as the Macbeth ColorChecker shown here. Patches A and B are those selected to be highly contrasting with each other for case (1). For case (2), the reflectance of patch A is copied to the location of patch B, creating two patches with identical spectra next to each other separated by a black border. (b) Reflectance spectra of patches A and B.

B. Mathematical Similarity of Two Spectra

It is often useful to assess the similarity (or dissimilarity) of two spectra without referencing a biological visual system [8]. In this paper, the mathematical dissimilarity between the pure and recorded version of a spectrum was used as an objective measure of contamination, which was quantified using the spectral angle mapper (SAM) metric [23]:

$$\theta_{\mathrm{SAM}} = \cos^{-1}\frac{S_A^T S_B}{\|S_A\|\|S_B\|}. \tag{7}$$

Here, spectra are treated as two high-dimensional vectors (S_A, S_B). The angle between the vectors can be thought of as a measure of alignment; the smaller the angle, the more similar the two spectra are in shape. This metric is insensitive to differences in magnitude.

C. Modeling of Color Discriminability

One of the methods frequently used to assess discriminability of colors in animal vision is the *receptor noise* model developed by Vorobyev and Osorio [24]. In the absence of perceptual thresholds for the visual systems of most animals, this model predicts color discriminability by assuming that thresholds are set by color opponency mechanisms whose performance is limited by receptor noise. For a visual system with n receptor channels, color is encoded with $n-1$ opponent mechanisms; the achromatic signal is disregarded and the relative proportion of each receptor determines the receptor noise. Similar to the CIE LAB-based distance metrics, two color stimuli are indistinguishable if the distance between them is one just noticeable difference (JND) or less. According to this model, color contrast (ΔS) for a dichromat visual system is computed as follows [10]:

$$(\Delta S)^2 = \frac{(\Delta Q_1 - \Delta Q_2)^2}{e_1^2 + e_2^2}, \tag{8}$$

and for a trichromat,

$$(\Delta S)^2 = \frac{e_1^2(\Delta Q_3 - \Delta Q_2)^2 + e_2^2(\Delta Q_3 - \Delta Q_1)^2 + e_3^2(\Delta Q_1 - \Delta Q_2)^2}{(e_1e_2)^2 + (e_1e_3)^2 + (e_2e_3)^2}, \tag{9}$$

where $\Delta Q_i = Q_{i,a} - Q_{i,b}$ is the difference between the quantum catch Q_i of a stimuli a and b in the ith photoreceptor type. Quantum catch is found by

$$Q_i = k\int_{\lambda_{\min}}^{\lambda_{\max}} I(\lambda)R(\lambda)S_i(\lambda)\mathrm{d}\lambda, \tag{10}$$

where $\lambda_{\min}$ and $\lambda_{\max}$ are the bounds of the light spectrum of interest, $I(\lambda)$ is the spectrum of the incident light, $R(\lambda)$ is the reflectance spectrum of the surface being measured, $S_i(\lambda)$ is the spectral sensitivity of receptor type i, and k is the von Kries adaptation constant, which is set to unity for this paper. The e_i in Eqs. (9) and (10) represents noise in receptor type i and can be approximated using the Weber fraction (w_i) [10]:

$$w_i = \left(\frac{0.05}{\sqrt{n_i}}\right)\sqrt{n_{lws}}, \tag{11}$$

where n_i is the estimate of the proportion of the ith wavelength sensitive cone (i.e., short, medium, or long), and n_{lws} is the estimate of the proportion of the long wavelength sensitive cones [10].

The visual system parameters for the poison dart frog are taken from [20] ($\lambda_{\max,S,M,L} = 470,\ 489,\ 561$ nm $n_{lws} = 4$, $n_{mws} = 3$, $n_{sws} = 1$) and those for the ferret are from [11] ($\lambda_{\max,S,L} = 430,\ 558$ nm $n_{lws} = 14$, $n_{sws} = 1$). The spectral sensitivities corresponding to the $\lambda_{\max}$ values were calculated as described in [8].

4. RESULTS

In this section, the effect of d and α on the spectral content of a signal is investigated by comparing the signal to its uncontaminated reflectance spectrum mathematically (Section 4.A) and perceptually relative to two visual systems (Section 4.B). For simplicity, it is assumed that the spectral measurements for the test stimuli are taken with the tip of the fiber pointing to the center of each patch, and that when measurements for two patches are being compared, they are recorded at the same d and α. This is a simplifying assumption and is unlikely to hold in a real life case (especially when taking measurements from animals in the wild).

A. Mathematical Similarity of Spectra

In Fig. 4(a), cross sections of the cone of acceptance are shown for two measurement angles that are commonly used in animal coloration measurements, 90° (cross sections are circles) and 45° (cross sections are ellipses), respectively, with the measurement distance varying from 0 to 20 cm. The upper limit of 20 cm was chosen based on the author's experience—in general, measurements taken from distances farther than this are excluded from scientific analyses. In each case, it is assumed that the tip of the fiber is pointed at the center of patch A. Results vary little by fiber size; therefore, they are only shown for the 100 μm fiber in the rest of the paper. In Fig. 4(b), the similarity of the "contaminated" spectra of patches A and B relative to their "uncontaminated" versions [from Fig. 3(b)] are shown using SAM [Eq. (7)] for both measurement angles. The simulated patches are squares of 4.1 cm, with a black boundary separating them, and in both the conspicuous and camouflaged cases, the signal remains uncontaminated up to a measurement distance of about 10 cm. Beyond that, the cross-sectional sampling area expands into neighboring patches, and there are two points to note. First, for a given measurement distance, the degree of signal contamination depends on the measurement angle; the 45° measurement has higher SAM values (i.e., more dissimilarity) than the 90° measurement at any given distance. Second, the degree of contamination of spectra is not just a function of d and α but also of the neighboring colors. Patches A and B have different neighboring patches. The reflectance spectrum of patch B is more similar to the spectra of the patches that happen to be immediately adjacent to it than patch A is to its neighbors. This is purely a result of the arrangement of color patches on the synthetic test target and affects the overall SAM scores for the self-similarity of patches A and B.

The same analysis is repeated with the spectra in patch B replaced with a copy of patch A to simulate an example where an animal might be trying to match the colors of its

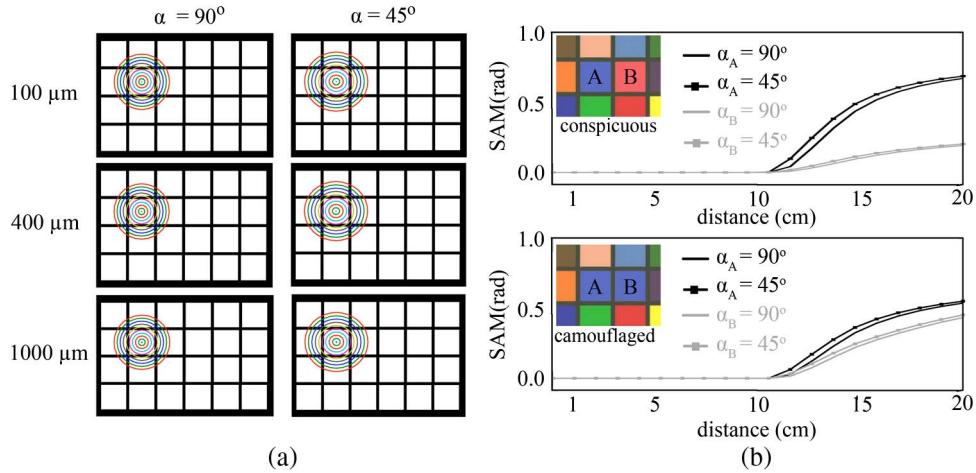

Fig. 4. (a) When the optical fiber (NA = 0.22) is held at 90° to the surface being measured, the cross section of the cone of acceptance is a disk. As the measurement distance increases, the radius of the disk also increases. For a measurement at 45°, the cross section is an ellipse. The concentric curves show cross sections at distances 0–20 cm, in ten equal steps. (b) Mathematical similarity of patches A (black lines) and B (gray lines) to their uncontaminated versions. Note that SAM only measures the similarity of the shape of the two spectra disregarding magnitude. Results for different fiber diameters were similar, and so only those for 100 μm are shown here.

background to fool predators. Originally, patch A had little spectral similarity to patch B. Now, patch A has a neighbor with an identical spectrum, and its overall level of contamination falls compared to that in the conspicuous case. The new patch B (blue), however, has less spectral overlap with its neighbors than did the old patch B (red, case 1), and its overall level of contamination increases. This demonstrates that the measurement distance and angle alone are not enough to predict the level of contamination of a color signal recorded with a certain optical fiber, and that the neighboring colors, which

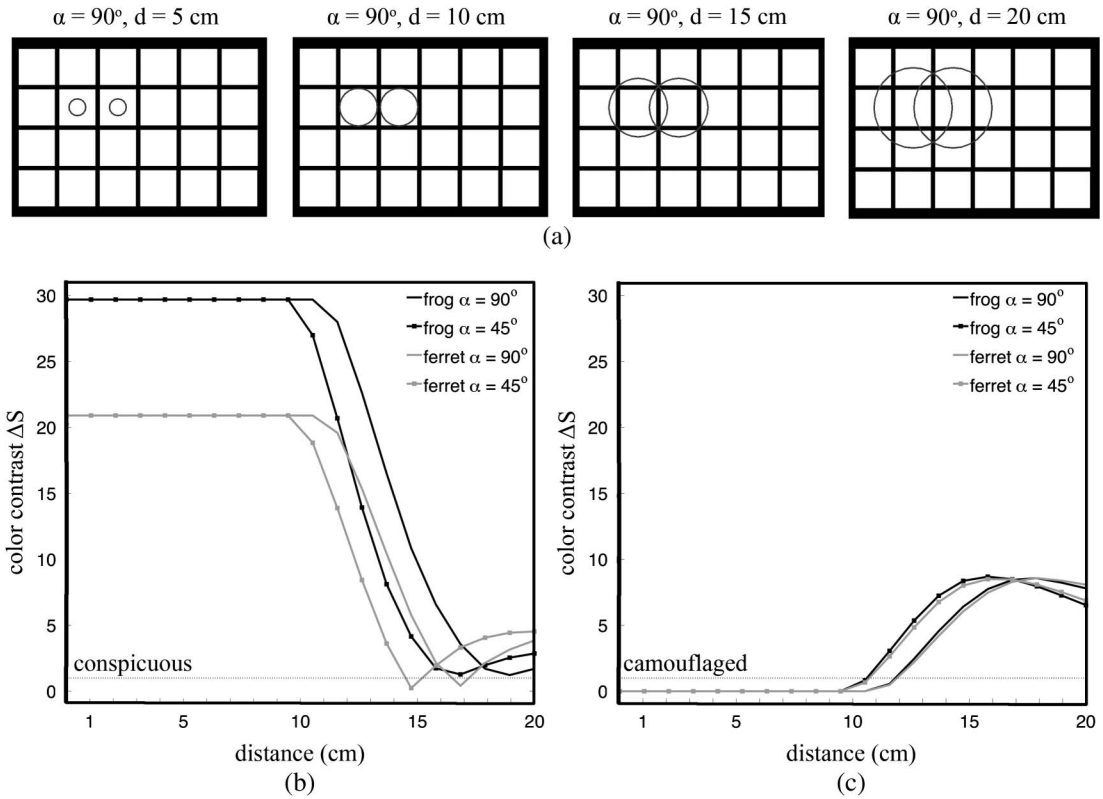

Fig. 5. (a) Cross section of the cone of acceptance when the fiber is held at an angle perpendicular to the surface, at measurement distances 5, 10, 15, and 20 cm (the dimension of each square is 4.1 cm). The signals measured from patches A and B are expected to remain pure up to $d = 10$ cm. (b) In the conspicuous case, patches A and B have little spectral overlap, and that translates to a high color contrast (ΔS) value for both the frog and the ferret. Beyond $d = 10$ cm, the color contrast decreases (the signals become more similar) with both distance and measurement angle. (c) In the camouflaged case, the spectrum of patch A is copied to the location of patch B. The color contrast is zero until $d = 10$ cm and after that, the spectra quickly get contaminated. The signals measured at $\alpha = 90°$ remain slightly more pure than at $\alpha = 45°$. The dashed line indicates the JND threshold of 1.

are often difficult to predict in a biological application, also play a role.

B. Perceptual Similarity of Spectra

1. Case (1): Conspicuous Animal

Patches A and B were chosen to represent the pattern of a conspicuous animal because they have little spectral overlap. The receptor noise model would be expected to predict a high color contrast between these patches in the eyes of both the dichromatic ferret and the trichromatic frog. Figure 5(a) shows the cross sections of the cone of acceptance for the measurement of patches A and B at distances $d = 5$, 10, 15 and 20 cm. Beyond $d = 10$ cm, the disks outgrow the square patches, and we expect the spectral content of each patch to become contaminated with spectra from neighboring patches. This in turn affects the color contrast between the patches. This is indeed the case as seen in Fig. 5(b); the color contrast (ΔS) values for both animals are well above the JND threshold of 1 (indicated by the dashed horizontal line) until $d = 10$ cm, but the two spectra become increasingly similar (for both the frog and the ferret) after that point. If these measurements were taken at a distance of 15 cm, the data could have led to an incorrect conclusion that the blue and red colors were indistinguishable (JND < 1) to the ferret. Note that the ΔS for the frog never falls below the JND $= 1$ line, meaning that these two patches, despite their spectral contamination, remain distinguishable to the trichromatic animal, which has the advantage of having an extra photoreceptor compared to the dichromate.

2. Case (2): Camouflaged Animal

For the case of a perfectly camouflaged animal, patches A and B have identical reflectance spectra but they have different neighboring colors [see Figs. 4(b) and 4(c) inset]. As expected, the spectra of patches remain identical when the measurements are uncontaminated, up to $d = 10$ cm, and for both animals the color contrast is zero [Fig. 5(c)]. Beyond that point, the contrast between the spectra measure at $\alpha = 90°$ remain lower for a slightly higher d value than it does for $\alpha = 45°$. Note that for this example, the magnitude of the color contrast for both visual systems are comparable, implying that the measurements of patch spectra (even though they are identical) are contaminated enough beyond $d = 11$ cm that the colors become distinguishable (JND > 1) to both the ferret and the frog.

5. DISCUSSION

In this work, the parameters of the elliptical cross section of the cone of acceptance of an optical fiber were derived [Eqs. (2)–(6)] for a fiber of known diameter and NA held at a distance d and angle α. The effect of varying d and α on spectral signal quality was investigated using SAM, a purely mathematical measure of spectral shape similarity, and the Vorobyev–Osorio receptor noise model [24], a perceptual measure of color discriminability. Visual systems of a trichromatic frog and a dichromatic ferret were chosen as examples. Animal vision models other than the receptor noise model also take as input full spectral signals (rather than consumer camera photographs that do not represent spectra), so the approach presented here can be extended to any such model. Furthermore, since the equation of the ellipse representing the intersection of the acceptance cone and a surface only depends on the fiber diameter and NA, which are provided by manufacturers, this method is generalizable to applications of spectroscopy in other fields.

It was shown here that signal contamination varied based on the spectral content of the neighboring colors of a patch in addition to the measurement distance, which was more important than the measurement angle for the two angles considered (45° and 90°). The measurement angle simulated here did not appear to have a large effect on the color measurement, but 90° may be preferable if the shape being measured is square. Fiber size, at least in the range of 100–1000 μm, had a negligible effect on the field of view of the fiber. The patches used in this example were squares of 4.1 cm, and for a feature of that size and shape, the maximum measurement distance that produced pure colors was approximately 10 cm. Most features measured in the context of animal coloration are smaller than 4.1 cm; for example, the poison frog is only 1–2 cm in size [20], and the largest body component of a European cuttlefish of mantle length 20 cm was around 3 cm [8]. Animals often have splotchy patterns with irregular shapes and non-Lambertian skins, and even though it may be possible to know the size of a feature that will be measured, there may be no *a priori* information regarding its neighboring colors. Equations (2)–(6) presented in this paper could be used as guidelines before spectral measurements from animals or their habitats are made. If that is not possible, they can be used to assess the possible level of signal contamination *after* the study, provided the measurement angle and distance were documented. Quantifying the degree of contamination is important because even for solid color patches of relatively large dimensions, as used in this paper, it is possible to obtain color contrast values that are misleading enough to conclude that two colors with little spectral overlap would be indistinguishable to a visual system.

APPENDIX A

Proof. In three-space, $((x^2 + y^2)/(R/H)^2) = z^2$ defines a right cone with its apex on the origin $O(0, 0, 0)$, whose base is a circle with radius R in the XY plane located at a distance H away from the apex along the z direction. A plane that intersects this cone at height H_s, at an angle α is defined by $z = \tan\alpha \cdot y + H_s$. These two equations are solved together to find their intersection:

$$\frac{x^2 + y^2}{\left(\frac{R}{H}\right)^2} = (\tan\alpha \cdot y + H_s)^2.$$

Expanding the terms on the right-hand side and rearranging gives

$$\frac{x^2}{\left(\frac{R}{H}\right)^2} + y^2\left(\frac{1}{\left(\frac{R}{H}\right)^2} - \tan^2\alpha\right) - 2\tan\alpha H_s y = H_s^2.$$

Defining $t = R/H$ and $M = (1/t^2) - \tan^2\alpha$ yields

$$\frac{x^2}{Mt^2} + y^2 - \frac{2\tan\alpha H_s}{M}y = \frac{H_s^2}{M}.$$

Completing the square, the last equation reduces to

$$\frac{x^2}{Mt^2C} + \frac{\left(y - \frac{H_s \tan\alpha}{M}\right)^2}{C} = 1,$$

where $C = (H_s^2/M)(1 + (\tan^2\alpha/M))$. From this, we obtain the center of the ellipse as $(x_c, y_c) = (0, (H_S \tan\alpha/(1/t^2) - (\tan\alpha)^2))$, with semi-major axis $a = \sqrt{C(1 - t^2(\tan\alpha)^2)}$ and semi-minor axis $b = \sqrt{C}$. A quick check shows that when $\alpha = 0 (x_c, y_c) = (0, 0)$ and $a = b = \sqrt{C}$, making a circle parallel to the base of the cone.∴

ACKNOWLEDGMENTS

Lonny Lippsett and Dr. Chris Reddy's (WHOI) lectures provided inspiration and motivation for this paper. The author would like to thank all members of Rosenholtz (MIT) and Hanlon (MBL) Laboratories, notably Dr. Lydia Mäthger for her mentorship and scientific support. Dr. Lydia Mäthger, Dr. Nick Loomis, Dr. Cassie Stoddard, and two anonymous reviewers provided invaluable comments on various drafts. Funding for this work was provided by the Grant No. NIH-NEI EY021473 to R. Rosenholtz.

REFERENCES

1. D. Brainard, "Color vision theory," in *International Encyclopedia of the Social and Behavioral Sciences*, N. Smelser and P. Baltes, eds. (Elsevier, 2001), pp. 2256–2263.
2. M. E. Maan and M. E. Cummings, "Female preferences for aposematic signal components in a polymorphic poison frog," Evolution **62**, 2334–2345 (2008).
3. A. Kelber, M. Vorobyev, and D. Osorio, "Animal colour vision, behavioural tests and physiological concepts," Biol. Rev. **78**, 81–118 (2003).
4. M. C. Stoddard and M. Stevens, "Avian vision and the evolution of egg color mimicry in the common cuckoo," Evolution **65**, 2004–2013 (2011).
5. J. A. Endler and P. W. Mielke, Jr., "Comparing entire colour patterns as birds see them," Biol. J. Linn. Soc. **86**, 405–431 (2005).
6. G. Wyszecki and W. S. Stiles, *Color Science: Concepts and Methods, Quantitative Data, and Formulae*, 2nd ed. (Wiley, 2000).
7. D. Akkaynak, T. Treibitz, B. Xiao, U. A. Gurkan, J. J. Allen, U. Demirci, and R. T. Hanlon, "Use of commercial off-the-shelf (COTS) digital cameras for scientific data acquisition and scene-specific color calibration," J. Opt. Soc. Am. A (to be published).
8. D. Akkaynak, J. Allen, L. Mäthger, C.-C. Chiao, and R. Hanlon, "Quantification of cuttlefish (Sepia officinalis) camouflage: a study of color and luminance using *in situ* spectrometry," J. Comp. Physiol. A **199**, 211–225 (2013).
9. R. T. Hanlon, C.-C. Chiao, L. M. Mäthger, and N. J. Marshall, "A fish-eye view of cuttlefish camouflage using in situ spectrometry," Biol. J. Linn. Soc. **109**, 535–551 (2013).
10. C. C. Chiao, J. K. Wickiser, J. J. Allen, B. Genter, and R. T. Hanlon, "Hyperspectral imaging of cuttlefish camouflage indicates good color match in the eyes of fish predators," Proc. Natl. Acad. Sci. USA **108**, 9148–9153 (2011).
11. L. A. Isaac and P. T. Gregory, "Can snakes hide in plain view? Chromatic and achromatic crypsis of two colour forms of the Western terrestrial garter snake (Thamnophis elegans)," Biol. J. Linn. Soc. **108**, 756–772 (2013).
12. S. D. Finkbeiner, A. D. Briscoe, and R. D. Reed, "The benefit of being a social butterfly: communal roosting deters predation," Proc. R. Soc. B **279**, 2769–2776 (2012).
13. O. Lind, M. Mitkus, P. Olsson, and A. Kelber, "Ultraviolet sensitivity and colour vision in raptor foraging," J. Exp. Biol. **216**, 1819–1826 (2013).
14. M. E. Maan and M. E. Cummings, "Poison frog colors are honest signals of toxicity, particularly for bird predators," Am. Nat. **179**, E1–E14 (2012).
15. S. M. Bybee, F. Yuan, M. D. Ramstetter, J. Llorente-Bousquets, R. D. Reed, D. Osorio, and A. D. Briscoe, "UV photoreceptors and UV-yellow wing pigments in *Heliconius* butterflies allow a color signal to serve both mimicry and intraspecific communication," Am. Nat. **179**, 38–51 (2012).
16. F. Cortesi and K. Cheney, "Conspicuousness is correlated with toxicity in marine opisthobranchs," J. Evol. Biol. **23**, 1509–1518 (2010).
17. N. Langmore, M. Stevens, G. Maurer, and R. Kilner, "Are dark cuckoo eggs cryptic in host nests?" Anim. Behav. **78**, 461–468 (2009).
18. J. Baldwin and S. n. Johnsen, "The male blue crab, *Callinectes sapidus*, uses both chromatic and achromatic cues during mate choice," J. Exp. Biol. **215**, 1184–1191 (2012).
19. O. Nokelainen, R. H. Hegna, J. H. Reudler, C. Lindstedt, and J. Mappes, "Trade-off between warning signal efficacy and mating success in the wood tiger moth," Proc. R. Soc. B **279**, 257–265 (2012).
20. A. Siddiqi, T. W. Cronin, E. R. Loew, M. Vorobyev, and K. Summers, "Interspecific and intraspecific views of color signals in the strawberry poison frog *Dendrobates pumilio*," J. Exp. Biol. **207**, 2471–2485 (2004).
21. M. Bass, C. DeCusatis, J. Enoch, V. Lakshminarayanan, G. Li, C. Macdonald, V. Mahajan, and E. Van Stryland, *Handbook of Optics, Volume II: Design, Fabrication and Testing, Sources and Detectors, Radiometry and Photometry* (McGraw-Hill, 2009).
22. M. D. Fairchild and G. M. Johnson, "METACOW: a public-domain, high-resolution, fully-digital, noise-free, metameric, extended-dynamic-range, spectral test target for imaging system analysis and simulation," in *Color and Imaging Conference* (Society for Imaging Science and Technology, 2004), pp. 239–245.
23. R. H. Yuhas, A. F. H. Goetz, and J. W. Boardman, "Discrimination among semiarid landscape endmembers using the spectral angle mapper (SAM) algorithm," in *Summaries of the Third Annual JPL Airborne Geoscience Workshop*, Pasadena, California (1992), Vol. **1**, pp 147–149.
24. M. Vorobyev and D. Osorio, "Receptor noise as a determinant of colour thresholds," Proc. R. Soc. B **265**, 351–358 (1998).